The most interesting result is that the same information also could be obtained with the model-based interpretation of the SPECT scan, thus avoiding the cumbersome and expensive pharmacologic protocol described above. Indeed, assuming the receptor model is used, the simple observation of the temporal behavior to the ROI_T/ROI_{NT} ratio gives strong evidence that tumor uptake was specific.

Therefore, we suggest pentetreotide can be extended beyond its use as a tumor detection agent to that of a tumor characterizing agent, which increases the clinical importance of the scintigraphic data and may provide direction for therapeutic management. This aim probably will be best fulfilled by true quantitative approaches (*8*), but the simplicity of the method we propose can represent a reasonable trade-off in clinical management. Future developments of SSR2 receptor tracers, labeled with more favorable isotopes (*9*) and with high-resolution SPECT instrumentation, can further increase the value of the biological in vivo characterization of SSR2-expressing tumors.

REFERENCES

1. Krenning EP, Kwekkeboom DJ, Bakker WH, et al. Somatostatin receptor scintigraphy with ^{111}In-DTPA-D-Phe- and ^{123}I-Tyr-octreotide. The Rotterdam experience with more than 1000 patients. *Eur J Nucl Med* 1993;8:715–731.
2. Lamberts SWJ, Krenning EP, Reubi JC, et al. The role of sandostatin and its analogs in the diagnosis and treatment of tumors. *Endocr Rev* 1991;4:450–482.
3. Peri A, Cordellea-Niele E, Miele L, Mukherje AB. Tissue-specific expression of the gene coding for human clara cell 10-kD protein: a phosphoerpase A_2-inhibitory protein. *J Clin Invest* 1993;92:2099–2109.
4. Maini CL, Tofani A, Venturo I, et al. Somatostatin receptor imaging in small cell lung cancer using ^{111}In-DTPA-D-Phe-octreotide: a preliminary study. *Nucl Med Commun* 1993;14:962–968.
5. Innis RB, Al-Tikriti MS, Zoghbi SS, et al. SPECT imaging of the benzodiazepine receptors: feasibility of in vivo potency measurement from stepwise displacement curves. *J Nucl Med* 1991;9:1754–1761.
6. Morlein SM, Welch MS. Application of SPECT to the in vivo measurement of benzodiazepine potency. *J Nucl Med* 1991;9:1762–1763.
7. Lassen NA. Neuroreceptor quantitation in vivo by the steady-state principle using constant infusion or bolus injection of radioactive tracers. *J Cereb Blood Flow Metab* 1992;5:709–716.
8. Eckelman WC. The application of receptor theory to receptor-binding and enzyme-binding oncologic radiopharmaceuticals. *Nucl Med Biol* 1994;5:759–769.
9. Bakker WH, Krenning EP, Reubi JC, et al. In vivo application of [^{111}In-DTPA-D-Phe]-octreotide for detection of somatostatin receptor-positive tumors in rats. *Life Sci* 1991;49:1593–1601.

Influence of Chemotherapy on FDG Uptake by Human Cancer Xenografts in Nude Mice

Takashi Yoshioka, Hiromu Takahashi, Hirosuke Oikawa, Syunichi Maeda, Tatuo Ido, Takashi Akaizawa, Hiroshi Fukuda and Ryunosuke Kanamaru

Department of Clinical Oncology, Nuclear Medicine and Radiology, Institute of Development, Aging and Cancer and Cyclotron and Radioisotope Center, Tohoku University, Sendai, Japan

This study evaluated the use of PET with ^{18}F-2-deoxy-2-fluoro-D-glucose (^{18}F-FDG) for monitoring chemotherapy effects, using a human cancer xenograft (poorly differentiated human gastric cancer) in vivo model. **Methods:** Tumor ^{18}F-FDG uptakes and sizes were measured after administrating mitomycin (MMC), cisplatin (CDDP) and adriamycin (ADR) to xenograft-bearing nude mice and compared with ^{18}F-FDG tumor uptake and tumor size in a non-therapy group. The correlation between the uptake and size was also assessed. **Results:** The largest reduction in tumor size after chemotherapy occurred in the MMC administered group, followed by the CDDP case, with no reduction in the ADR group as compared to the controls. Fluorine-18-FDG tumor uptake after chemotherapy was also decreased in the MMC and CDDP groups, in that order, but not in the ADR case. With MMC and CDDP, size reduction became significant on Days 8 or 11, whereas ^{18}F-FDG tumor uptake had already been decreased on Days 3 or 7. **Conclusion:** Fluorine-18-FDG uptake decreases in parallel to the efficacy of anticancer agents and correlates with subsequent morphologic changes. We conclude that ^{18}F-FDG PET tumor images are indeed useful for monitoring the effects of cancer chemotherapy.

Key Words: fluorine-18-FDG; human cancer xenograft; PET; chemotherapy

J Nucl Med 1997; 38:714–717

With cancer chemotherapy, it is important to choose the most effective chemotherapeutic agents for individual patients. There have been several attempts to develop in vitro (*1–6*) and in vivo (*7,8*) systems that would predict the response of a tumor, in an individual patient, to a particular chemotherapeutic agent, but the results have been far from satisfactory. In clinical practice, the chemotherapist chooses chemotherapeutic agents on the basis of his experience and by monitoring morphological changes of tumors by physical examination, radiograph studies, endoscopy, CT, US or MRI, in a continuous decision-making process.

The development of PET has made it possible to study the metabolism of cancer tissues. The positron-labeled compound ^{18}F-2-deoxy-2-fluoro-D-glucose (^{18}F-FDG) is widely used in PET as a tracer for glucose metabolism (*9*) because it is phosphorylated by hexokinase but essentially cannot be further metabolized, becoming preferentially trapped in the cells (*10*). As enhanced glycolysis is one of the best-documented characteristics of malignant tumors (*11*), ^{18}F-FDG PET has been used for successful imaging of various kinds of human neoplasms (*12–19*).

Theoretically, ^{18}F-FDG PET should also be suitable for follow-up after cancer treatment, since its uptake relates to the number of viable tumor cells (*20*). The response of tumors to chemotherapy might, therefore, be recordable earlier and more exactly in terms of ^{18}F-FDG uptake than from morphological changes. Several clinical studies using ^{18}F-FDG have been performed to evaluate therapeutic response in malignant tumors (*14–17, 21–24*) and there also have been reports of experimental studies concerned with the relationship between treatment efficacy and ^{18}F-FDG uptake (*25,26*). However, detailed experimental in vivo studies on the correlation between morphologic alterations and ^{18}F-FDG uptake in tumors caused by chemotherapy have been lacking.

In this study we compared the relationship between tumor

Received Jan. 11, 1996; revision accepted Jul. 19, 1996.

For correspondence or reprints contact: Takashi Yoshioka, MD, Department of Clinical Oncology, Institute of Development, Aging and Cancer, Tohoku University, 4–1, Seiryo-machi, Aoba-ku, Sendai 980-77, Japan.

volume and ^{18}F-FDG uptake after chemotherapy using human cancer xenografts.

MATERIALS AND METHODS

Xenografts

The SC-6-JCK used in this study is a poorly differentiated human gastric adenocarcinoma cell line. It was supplied as an established xenograft in a nude mouse and serially transplanted in nude mice at our institution.

Tumor tissue fragments, approximately 2 mm^2, were inoculated into the subcutaneous tissue of the backs of inbred 5-wk-old male BALB/c nu/nu mice maintained under pathogen-free conditions.

Radiopharmaceutical

Fluorine-18–2-deoxy-2-fluoro-D-glucose was synthesized by the method described by Shiue (*27*). The specific activity varied according to the integrated cyclotron beam dose focused on the target and ranged from 1–10 mCi/mg at the end of synthesis. Radiochemical purity was 97%–98%.

Chemotherapeutic Agents

Commercially available mitomycin C (MMC), adriamycin (ADR) and cisplatin (CDDP) were used for the experiment. MMC and ADR were dissolved in about 0.2 ml of physiological saline and CDDP was dissolved in about 0.2 ml of distilled water. MMC and CDDP were administered once intraperitoneally, and ADR once intravenously because it is poorly absorbed by the peritoneum. The administered doses were 6 mg/kg for MMC, 8 mg/kg for CDDP and 8 mg/kg for ADR, which were previously described as adequate doses for treatment (*28*).

Measurement of Tumor Size and Treatment

Tumors inoculated into the subcutaneous tissue of the backs of nude mice were measured (length and width) with sliding calipers every day by the same person. Using the method of Geran et al. (*29*), the tumor volume (V) in mm^3 was calculated from the linear measurements using the formula: tumor volume (mm^3) = length (mm) × (width (mm))^2/2. On the 16th day after inoculation, when tumors had reached 300–500 mm^3, tumor-bearing mice were randomized into four test groups (MMC, CDDP, ADR and control). The relative mean tumor volume (RV) was calculated as Vi/Vo, where Vi is the mean tumor volume of a group at any given time and Vo is the mean tumor volume at the initial treatment. Growth curves after treatment were generated from the calculated RV.

Radioactivity Measurement

Six ^{18}F-FDG tissue distribution studies were performed at 1, 3, 5, 7, 10 and 14 days after treatment. Each study encompassed four test groups, each consisting of five to seven nude mice (MMC, CDDP, ADR and control). Fluorine-18-FDG was dissolved in isotonic saline and approximately 20 μCi/0.2 ml were injected intravenously through the lateral tail vein. The mice were killed by decapitation 60 min after the injection and the tumors removed and blotted. The tumors were weighed and counted in an automated NaI well counter along with a standard sample of the injected ^{18}F-FDG. Radioactivity was corrected for decay and data were expressed as the differential uptake ratio (DUR):

$$\text{DUR} = \frac{\text{tissue counts/tissue weight}}{\text{injected dose counts/body weight.}}$$

Statistical Comparison

The Student's t-test was used for determining the statistical significance of differences between tumor volumes and in uptake data.

RESULTS

The growth curves after treatment are shown in Figure 1.

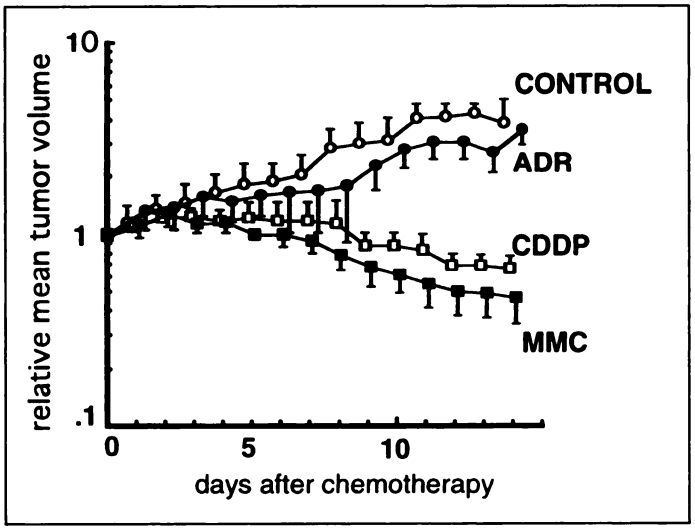

FIGURE 1. Tumor growth curves after chemotherapy. Symbols are mean values and bars are s.d. The tumor proved sensitive to MMC and CDDP, in that order, and not to ADR.

Each curve gives the mean and s.d. of the relative tumor volume. The relative tumor volumes on Day 14 were 0.46 ± 0.21 for MMC, 0.66 ± 0.10 for CDDP, 3.54 ± 0.57 for ADR and 3.85 ± 1.23 for the control group. Reduction of tumor size was largest in the MMC administered group, followed by the CDDP case, although no significant difference was observed between the two ($p < 0.1$; Student's t-test). The ADR-treated group demonstrated no reduction. In the MMC group, reduction was evident on Day 4, which became significant on Day 8 (RV = 0.78 ± 0.13) as compared with the initial volume ($p < 0.01$). Likewise for the CDDP group, where tumor reduction was noted on Day 5 and with significance from Day 11 (RV = 0.83 ± 0.17) ($p < 0.01$), when the relative tumor volume was smaller than just before the treatment commencement.

Data for tumor uptake of ^{18}F-FDG in each drug administration group and the controls are shown in Table 1, and drug response curves in Figure 2. There was a gradual and constant decrease in uptake from Day 1 to Day 7 with a slight increase from Day 7 to Day 14 in the MMC and CDDP groups, but there was a slight decrease from Day 1 to Day 5 and a gradual

TABLE 1
Fluorine-18-FDG Tumor Uptake after Chemotherapy

Day	Differential uptake ratio			
	Control	ADR	CDDP	MMC
1	1.44 ± 0.32 (6)*	1.43 ± 0.22 (5)	1.26 ± 0.06 (5)	1.24 ± 0.18 (6)
3	1.36 ± 0.30 (6)	1.27 ± 0.37 (5)	1.26 ± 0.14† (5)	0.96 ± 0.27‡ (7)
5	1.44 ± 0.40 (5)	1.20 ± 0.45 (5)	1.01 ± 0.16† (6)	0.85 ± 0.29‡ (6)
7	1.35 ± 0.32 (6)	1.26 ± 0.23 (6)	0.93 ± 0.21‡¶ (5)	0.71 ± 0.22§** (7)
10	1.41 ± 0.21 (7)	1.32 ± 0.22 (5)	0.97 ± 0.22§¶ (5)	0.85 ± 0.12§* (5)
14	1.33 ± 0.19 (7)	1.39 ± 0.14 (5)	1.10 ± 0.24†¶ (6)	0.88 ± 0.20§** (5)

Values are mean ± s.d.
*Number of nude mice.
†$p < 0.1$, ‡$p < 0.05$ and §$p < 0.01$, compared with the control.
¶$p < 0.1$ and **$p < 0.01$ compared with the ADR case.

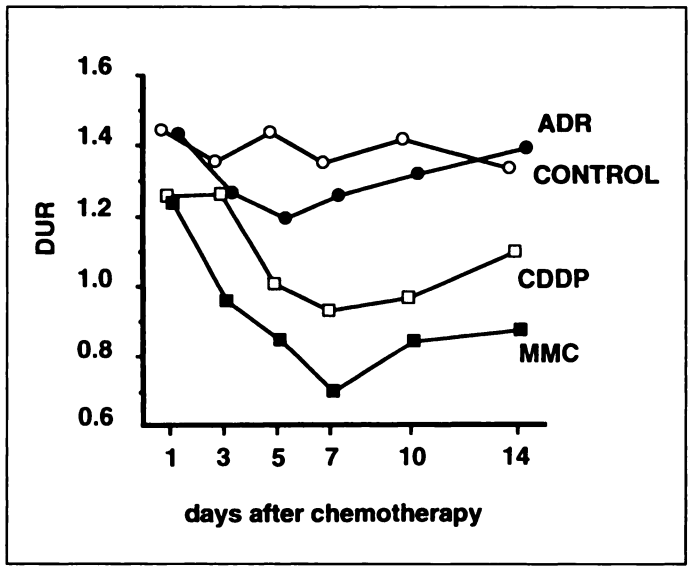

FIGURE 2. Time-response curves of ^{18}F-FDG tumor uptake after chemotherapy. Consistent decreases from Day 1 to Day 7 were observed in the sensitive drug groups, but not with ADR.

increase from Day 5 to Day 14 in the ADR case. Fluorine-18-FDG tumor uptake in the MMC-administered group showed a steady decrease that became significant in comparison with the control level on Day 3 ($p < 0.05$). In the CDDP case, a significant decrease was noted on Day 7 ($p < 0.05$). With both drugs the uptake values remained decreased at later time points (Table 1). Fluorine-18-FDG tumor uptake in the ADR-administered group demonstrated no difference from the control group, but the values were higher for the two other drugs from Day 7 to Day 14 (Table 1). Fluorine-18-FDG tumor uptake in the MMC group was consistently lower than that of the CDDP-administered group, but there was no statistically significant difference between the two.

DISCUSSION

PET using ^{18}F-FDG, a structural analog of glucose and labeled with the short-lived positron-emitting radioisotope ^{18}F, has provided a noninvasive methodology that can give quantitative information on regional glycolytic processes (*9,10*). As increased glycolysis is one of the most important characteristics of cancer cells (*11*), ^{18}F-FDG PET has been widely used for cancer diagnosis with successful imaging of various kinds of malignant tumors (*12–19*).

We find ^{18}F-FDG PET has two advantages. It facilitates diagnosis of tumor aggressivity because of the positive correlation between glycolytic rate and proliferative activity or histologic de-differentiation (*12,19,22,23,30,31*). Also, it is suitable for follow-up after cancer treatment because ^{18}F-FDG uptake reflects the viability of tumor cells (*20*).

Abe et al. (*25*) reported, using experimental murine cancer models, that ^{18}F-FDG uptake is reduced in radiosensitive but not radioresistant tumors and that metabolic changes lead to morphologic alterations in radiosensitive tumors after radiation. Minn et al. (*22*) reported that successful treatment causes a decrease in ^{18}F-FDG uptake in patients with head and neck tumors, and similar tendencies were also noted in patients with other tumors (*14–17,21,23,24*). In this study, a comparison of ^{18}F-FDG uptake and tumor size allowed a good correlation to be established after administration of anticancer drugs with differing efficacy against xenograft growth.

It was earlier shown that SC-6-JCK responds well to MMC, moderately to CDDP and poorly to ADR by Shimoyama et al. (*32*) and a previous study in our institute (*33*) and tumor size measurement in this study also gave similar results (Fig. 1). Our present findings show that ^{18}F-FDG uptake after chemotherapy is decreased in parallel to the response in terms of tumor growth and, thus, suggest that ^{18}F-FDG PET might be suitable for monitoring cancer chemotherapy.

The time response of ^{18}F-FDG uptake indicated the possibility of more rapid detection of chemotherapeutic potential than with tumor size. This was the case with both MMC and CDDP administration. The reason for this is presumably because cytotoxic effects of anticancer agents cause metabolic arrest of cancer cells, as reflected by ^{18}F-FDG uptake, before necrosis and reduction in tumor size can occur. The latter is also complicated by inflammatory changes and fibrosis. The observations in our study suggest that ^{18}F-FDG PET tumor imaging might allow the effectiveness of chemotherapy for an individual patient to be decided earlier than with conventional morphological methods.

In this study, ^{18}F-FDG uptakes in MMC- and CDDP-administered groups increased slightly after Day 7. We think that these phenomena show the possibility of the recurrence of cell proliferation.

The recent development of GCS-F and bone marrow transplantation (ABMT) has reduced the risk of infection induced by bone marrow suppression that is the most dangerous side effect of anticancer agents (*34*), making possible an increase in the dose intensity for high-dose chemotherapy (HDCT), which has augmented the number of long-term survivors with some kinds of cancers (*35*). Therefore, it is even more important now to identify effective chemotherapeutic agents for individual cancer patients. While many assays of chemosensitivity in vitro and in vivo have been developed, the in vitro results are generally affected by several experimental factors, including drug concentration and exposure time, as well as number of cells seeded and culture duration, and this makes interpretation of any correlation with in vivo clinical efficacy very difficult (*1–6*). The nude mouse method, one of in vivo assays, is expensive and the success of transplantation is not guaranteed (*7*). Another in vivo assay, the subrenal capsular assay, cannot exclude the influence of immune or endocrine host reactions (*8*). Therefore, no routine method has so far been established for assessing chemosensitivity at the individual patient level. In clinical practice, rapid and reliable evaluation of chemotherapeutic effects is of great assistance in determining the most favorable anticancer drug regimen. Since the data in this study indicate that ^{18}F-FDG tumor uptake is decreased in parallel with the efficacy of anticancer agents in causing size reduction, this approach might be particularly suitable for this purpose.

This is the first study on the correlation between morphologic alterations and ^{18}F-FDG uptake in tumors caused by chemotherapy. Heterogeneity of tumor tissue in terms of ^{18}F-FDG kinetics is a potential source of problems in interpreting ^{18}F-FDG PET images for assessment of response to chemotherapy. However, our observations provide evidence that ^{18}F-FDG PET imaging is indeed useful for follow-up after cancer chemotherapy.

ACKNOWLEDGMENTS

We thank the staff of the Cyclotron Radioisotope Center. This work was supported in part by Grants-in-Aid for Cancer Research 1–9 and 62S-1 from the Ministry of Health and Welfare, Scientific Research No.01570347 and a Grant-in Aid for specially promoted research No.0628211 from the Ministry of Education, Science and Culture.

REFERENCES

1. Mosmann T. Rapid colormetric assay for cellular growth and survival: application to proliferation and cytotoxity assays. *J Immunol Methods* 1983;65:55–63.
2. Kuzmits R, Aigiger P, Frass M, et al. Influence of cytostatics on ATP-levels of leukemic cells. *Adr Exp Med Biol* 1984;165:383–388.
3. Salmon SE, Alberts DS, Durie BGM, et al. Clinical correlations of drug sensitivity in the human stem cell assay: recent results. *Cancer Res* 1980;74:300–305.
4. Tanigawa N, Kern DH, Hikasa Y, Morton DL. Rapid assay for evaluating the chemosensitivity of human tumors in soft agar culture. *Cancer Res* 1982;42:2159–2164.
5. Weisenthal LM, Marden JA, Dill PL, Macaluso CK. A novel dye exclusion method for testing in vitro chemosensitivity of human tumors. *Cancer Res* 1983;43:749–757.
6. Hoffman RM, Connors KM, Meerson-Monosov AZ, Herrera H, Price JH. A general native-state method for determination of proliferation capacity of human normal and tumor tissues in vitro. *Proc Natl Acad Sci USA* 1989;86:2013–2017.
7. Povlsen CO, Jacobsen GK. Chemotherapy of a human malignant melanoma transplanted in the nude mouse. *Cancer Res* 1975;35:2790–2796.
8. Bogden AE, Haskell PM, Lepage DJ, Kelton DE, Cobb WR, Esber HJ. Growth of human xenografts implanted under the renal capsule of normal immunocompetent mice. *Exp Cell Biol* 1979;47:281–293.
9. Reivich M, Kuhl D, Wolf A, et al. The [^{18}F]fluorodeoxyglucose method for measurement of local cerebral glucose utilization in man. *Circ Res* 1979;44:127–137.
10. Gallagher BM, Flowler JS, Gutterson NI, MacGregor RR, Wan CN, Wolf AP. Metabolic trapping as a principle of radiopharmaceutical design: some factors responsible for the biodistribution of [^{18}F]2-deoxy-2-fluoro-D-glucose. *J Nucl Med* 1978;19:1154–1161.
11. Warburg O. On the origin of cancer cells. *Science* 1956;123:309–314.
12. Di-Chiro G. Positron emission tomography using [^{18}F]fluorodeoxyglucose in brain tumors. A powerful diagnostic and prognostic tool. *Invest Radiol* 1986;22:360–371.
13. Yonekura Y, Benua RS, Brill AB, et al. Increased accumulation of 2-deoxy-2-(F-18)F-fluoro-D-glucose in liver metastases from colon carcinoma. *J Nucl Med* 1982;23:1133–1137.
14. Abe Y, Matsuzawa T, Fujiwara T, et al. Clinical assessment of therapeutic effects on cancer using ^{18}F-2-fluoro-2-deoxy-D-glucose and positron emission tomography: preliminary study of lung cancer. *Int J Radiat Oncol Biol Phys* 1990;19:1005–1010.
15. Wahl RL, Zasadny K, Helvie M, et al. Metabolic monitoring of breast cancer chemohormonotherapy using positron emission tomography: initial evaluation. *J Clin Oncol* 1993;11:2101–2111.
16. Haberkorn U, Strauss LG, Dimitrakopoulou A, et al. Fluorodeoxyglucose imaging of advanced head and neck cancer after chemotherapy. *J Nucl Med* 1993;34:12–17.
17. Nagata Y, Yamamoto K, Hiraoka M, et al. Monitoring liver tumor therapy with [^{18}F]FDG positron emission tomography. *J Comput Assist Tomogr* 1990;14:370–374.
18. Bares R, Klever P, Hauptmann S, et al. F-18 fluorodeoxyglucose PET in vivo evaluation of pancreatic glucose metabolism for detection of pancreatic cancer. *Radiology* 1994;192:79–86.
19. Okada J, Yoshikawa K, Itami M, et al. Positron emission tomography using fluorine-18-fluorodeoxyglucose in malignant lymphoma: a comparison with proliferative activity. *J Nucl Med* 1992;33:325–329.
20. Higashi K, Clavo AC, Wahl RL. Does FDG uptake measure proliferative activity of human cancer cells? In vitro comparison with DNA flow cytometry and tritiated thymidine uptake. *J Nucl Med* 1993;34:414–419.
21. Takahashi H, Yamagichi K, Wakui A, et al. New approach to clinical evaluation of cancer chemotherapy using positron emission tomography with ^{18}F-FDG (2-deoxy-2-[^{18}F]fluoro-D-glucose). *Sci Res Inst Tohoku Univ* 1986;69:830–838.
22. Minn H, Paul R, Ahonen A. Evaluation of treatment response to radiation in head and neck cancer with fluorine-18 fluorodeoxyglucose. *J Nucl Med* 1988;29:1521–1525.
23. Minn H, Soini I. Fluorine-18-fluorodeoxyglucose scintigraphy in diagnosis and follow up of treatment in advanced breast cancer. *Eur J Nucl Med* 1989;15:61–66.
24. Ichiya Y, Kuwabara Y, Otsuka M, et al. Assessment of response to cancer therapy using fluorine-18-fluorodeoxyglucose and positron emission tomography. *J Nucl Med* 1991;32:1655–1660.
25. Abe Y, Matsuzawa T, Fujiwara T, et al. Assessment of radiotherapeutic effects on experimental tumors using ^{18}F-2-fluoro-2-deoxy-D-glucose. *Eur J Nucl Med* 1986;12:325–328.
26. Higashi K, Clavo AC, Wahl RL. In vivo assessment of 2-fluoro-2-deoxy-D-glucose, L-methionine and thymidine as agents to monitor the early response of a human adenocarcinoma cell line to radiotherapy. *J Nucl Med* 1993;34:773–779.
27. Shiue CY, Salvadori PA, Wolf AP, Fowler JS, MacGregor RR. A new improved synthesis of 2-deoxy-2-[^{18}F]fluoro-D-glucose from ^{18}F-labeled acetyl hypofluorite. *J Nucl Med* 1982;23:899–903.
28. Kondo T, Imaizumi M, Taguchi T, et al. A model for chemosensitivity determination of anticancer agents against human cancer using nude mice. *Jpn Cancer Chemother* 1987;14:680–686 (in Japanese).
29. Geran RI, Greenberg NH, Macdonald MM, Shumacher AM, Abbott BJ. Protocols for screening chemical agents and natural products against animal tumors and other biological systems. *Cancer Chemother Res* 1972;3:51–61.
30. Minn H, Joensuu H, Ahonen A, Klemi P. Fluorodeoxyglucose imaging: a method to assess the proliferative activity of human cancer in vivo. Comparison with DNA flow cytometry in head and neck tumors. *Cancer* 1988;61:1776–1781.
31. Yoshioka T, Takahashi H, Oikawa H, et al. Accumulation of 2-deoxy-2[^{18}F]fluoro-D-glucose in human cancer heterotransplanted in nude mice: comparison between histology and glycolytic status. *J Nucl Med* 1994;35:97–103.
32. Shimoyama Y, Kubota T, Inoue S, et al. Antitumor activity of cisplatin and carboplatin against human tumor xenografts serially transplanted into nude mice with reference to gastric carcinomas. *Jpn J Cancer Chemother* 1987;14:2682–2687.
33. Kikuchi H, Asamura M, Gamoh M, Matsushita T, Wakui A, Takahashi T. An experimental study on SRCA (subrenal capsule assay)–using some immunosuppressive maneuvers. *Jpn J Cancer Chemother* 1988;15:2257–2263.
34. Eder JP, Elias A, Shea TC, et al. A Phase I-II study of cyclophosphamide, thiotepa and carboplatin with autologous bone marrow transplantation in solid tumor patients. *J Clin Oncol* 1990;8:1239–1245.
35. Antman K, Ayash L, Elias A, et al. A Phase II study of high dose cyclophosphamide, thiopenta and carboplatin with autologous marrow support in women with measurable advanced breast cancer responding to standard-dose therapy. *J Clin Oncol* 1992;10:102–110.

Transcobalamin II Receptor Imaging via Radiolabeled Diethylene-Triaminepentaacetate Cobalamin Analogs

Douglas A. Collins and H.P.C. Hogenkamp

Department of Diagnostic Radiology, Mayo Clinic, Rochester; and Department of Biochemistry, University of Minnesota, Minneapolis, Minnesota

Rapidly dividing cells up-regulate the number of transcobalamin II receptors during DNA replication. We have developed diethylene-triaminepentaacetate (DTPA) cobalamin analogs for the purpose of imaging transcobalamin II receptors in malignant and nonmalignant tissue. **Methods:** Methyl-, adenosyl- and cyanocobalamin-b-(4-aminobutyl)-amide-DTPA analogs were synthesized. In vitro binding of the analogs to the transcobalamin proteins was assessed by the unsaturated vitamin B12 binding capacity assay and compared to DTPA and cyanocobalamin. The biodistribution of the ^{111}In-DTPA cobalamin analogs was measured at 24 hr after injection into sarcoma-bearing mice and non-tumor-bearing mice and pigs. **Results:** Methyl-, adenosyl- and cyanocobalamin-b-(4-aminobutyl)-amide-DTPA analogs and DTPA were 94.0%, 90.4%, 66.4%, and 3.6%, respectively, as efficient in binding to the transcobalamin proteins when compared to cyanocobalamin. At 24 hr after administration, the cobalamin analogs had 5–17 times and 20–29 times, respectively, the amount of uptake within the resected tissue samples and transplanted sarcomas when compared to ^{111}In-DTPA. **Conclusion:** The radiolabeled DTPA cobalamin analogs are biologically active. Preliminary animal studies suggest that the analogs could be effective in vivo transcobalamin II receptor imaging agents.

Key Words: receptor imaging; tumor-seeking agent; vitamin B12

J Nucl Med 1997; 38:717–723

Vitamin B12 (cyanocobalamin) has two coenzymatic functions in humans. Methylcobalamin serves as the cytoplasmic coenzyme for ^{5}N-methyltetrahydrofolate:homocysteine methyl transferase (methionine synthetase, EC 2.1.1.13), which cata-

Received Feb. 1, 1996; revision accepted Aug. 8, 1996.

For correspondence or reprints contact: Douglas A. Collins, MD, Mayo Clinic, 200 First Street SW, Rochester, MN 55905.